J Mater Sci (2011) 46:5702–5708
DOI 10.1007/s10853-011-5523-7

Large strain response in acceptor- and donor-doped $Bi_{0.5}Na_{0.5}TiO_3$-based lead-free ceramics

Jiaming Li · Feifei Wang · Chung Ming Leung · Siu Wing Or · Yanxue Tang · Xinman Chen · Tao Wang · Xiaomei Qin · Wangzhou Shi

Received: 31 December 2010 / Accepted: 2 April 2011 / Published online: 20 April 2011

Abstract Effects of Fe and La addition on the dielectric, ferroelectric, and piezoelectric properties of $Bi_{0.5}Na_{0.5}TiO_3$–$Bi_{0.5}Li_{0.5}TiO_3$–$BaTiO_3$–Mn ceramics were investigated. Similar to the doping effect in lead-based piezoelectric materials, here the Fe-doped ceramic created a hard effect with an improved mechanical quality factor (Q_m) $\sim$ 160, coercive field (E_c) $\sim$ 2.9 kV/mm, decreased dielectric constant $\left(\varepsilon_{33}^T/\varepsilon_0\right) \sim 803$, and loss ($\tan\delta$) $\sim$ 0.024 while the La-doped one indicated a soft feature with improved piezoelectric constant (d_{33}) $\sim$ 184 pC/N, $\varepsilon_{33}^T/\varepsilon_0 \sim 983$, $\tan\delta \sim 0.033$, and decreased $E_c \sim 2.46$ kV/mm. In addition, the temperature dependence of the ferroelectric hysteresis loops and strain response under unipolar electric field was also studied. Around the depolarization temperature T_d, large strain value was obtained with the normalized d_{33}^* up to $\sim$1,000 pC/N, which was suggested originated from the development of the short-range order or non-polar phases in the ferroelectric matrix. All these would provide a new way to realize high piezoelectric response for practical application in different temperature scale.

J. Li · F. Wang (✉) · Y. Tang · X. Chen · T. Wang · X. Qin · W. Shi
Key Laboratory of Optoelectronic Material and Device, Mathematics & Science College, Shanghai Normal University, Shanghai 200234, China
e-mail: f_f_w@sohu.com

C. M. Leung · S. W. Or
Department of Electrical Engineering, The Hong Kong Polytechnic University, Hung Hom, Kowloon, Hong Kong

Introduction

Lead-oxide-based piezoelectric materials, represented by the $Pb(Zr_{1-x}Ti_x)O_3$ (PZT), have been widely used in electromechanical devices such as sensors, actuators, and ultrasonic transducers due to their excellent piezoelectric and electromechanical properties [1, 2]. However, the toxicity of the lead and its high evaporation during sintering easily cause serious ecological problem. Environmental legislation in the European Union, parts of Asia, and the US demands elimination of toxic lead for these materials systems [3], which spurred a large effort in the research for new lead-free piezoelectric materials in the past few years [4–9]. As a promising candidate, sodium bismuth titanate ($Bi_{0.5}Na_{0.5}TiO_3$, BNT), discovered by Smolenskii et al. in 1960s [10], attracted much attention recently due to its strong ferroelectric polarization and high Curie temperature [11–13]. The crystal structure of BNT is rhombohedral at room temperature. The rhombohedral to tetragonal phase transition temperature, T_{R-T}, and the Curie temperature, T_C, are approximately 300 and 540 °C during the heating process, respectively [11]. Besides, the BNT has a depolarization temperature T_d and a maximum dielectric temperature T_m of 185 and 340 °C, respectively. Due to its high coercive field and electrical conductivity, pure BNT ceramic is hard to be completely poled to obtain desired piezoelectric and pyroelectric response [10]. In order to solve this problem, extensive BNT-based solid solutions were developed in recent years such as $Bi_{0.5}Na_{0.5}TiO_3$–$Bi_{0.5}K_{0.5}TiO_3$–$BaTiO_3$ (BNT–BKT–BT) [14–16], $Bi_{0.5}Na_{0.5}TiO_3$–$Bi_{0.5}Li_{0.5}TiO_3$–$BaTiO_3$ (BNT–BLT–BT) [17], which have attracted considerable attention because of greatly improved piezoelectric performances near the morphotropic phase boundary (MPB) between the ferroelectric rhombohedral and tetragonal phases. Nevertheless, the electrical properties of

these BNT-based systems are still far from satisfaction in terms of practical application. Further improvement of the piezoelectric response remains an important issue to be resolved.

In general, there are two approaches to improve sintering, microstructure, and ultimately, to substantially improve the electrical properties for various applications. One is through microstructure modification such as designing textured structure with certain orientation to obtain high piezoelectric response. <001>-oriented textured BNT-BT ceramic with high piezoelectric constant d_{33} of ~200 pC/N has been achieved [18]. The other one is through compositional modifications, which can be divided into two types in traditional PZT system: donor and acceptor doping. Both types have been verified to be able to modify the dielectric, ferroelectric, piezoelectric, and electromechanical response [19–21]. Typical donor doping is through substitution of more positive ions (such as Bi^{3+} or La^{3+}) onto the Pb^{2+}, or Nb^{5+} and Sb^{5+} onto Ti^{4+}, which could increase the dielectric and piezoelectric constants, electromechanical coupling coefficients, reduce the coercive field and ageing effects due to the formation of the perovskite A-site vacancies facilitating the motion of domain and domain walls. On the other hand, substitution of the host cations with lower valence ions, denoted as the acceptor doping, could generate the oxygen vacancies, leading to decreased dielectric constant, loss, and enhanced mechanical quality factor and coercive field. This is generally attributed to the formation of the internal bias field from the defect dipoles [1, 2, 21].

The donor and acceptor doping have been found to create significant effect on the domain motions and the electrical properties in the traditional PZT system [19–21]. Nevertheless, a combination research of the acceptor and donor doping effects on the new lead-free system is little reported [22]. In our previous study, a Li and Mn co-modified BNT-BT solid solution was developed and the phase diagram was established with different Li content [23]. High d_{33} and planar electromechanical coupling factors k_P of 172 pC/N and 0.34 have been obtained. In order to further improve the properties, here a small amount of 0.2 mol% Fe and La, which could generate the hard and soft effects [21, 22], respectively, were added into the $0.875Bi_{0.5}Na_{0.5}TiO_3$–$0.06Bi_{0.5}Li_{0.5}TiO_3$–$0.065BaTiO_3$–0.005Mn (BNLBMT0.06). The effects of Fe and La doping on the dielectric, ferroelectric, and piezoelectric properties were systematically studied and the intrinsic mechanism responsible for them was discussed. In addition, in present study a very large electric-field-induced strain and normalized d^*_{33} of ~0.4% and ~1,000 pC/N was obtained around the depolarization temperature under 4 kV/mm, substantially larger than the previous solid solutions $Bi_{0.5}Na_{0.5}TiO_3$–$BaTiO_3$ (BNT–BT) system of ~0.3% and 700 pC/N (under 4 kV/mm) [24].

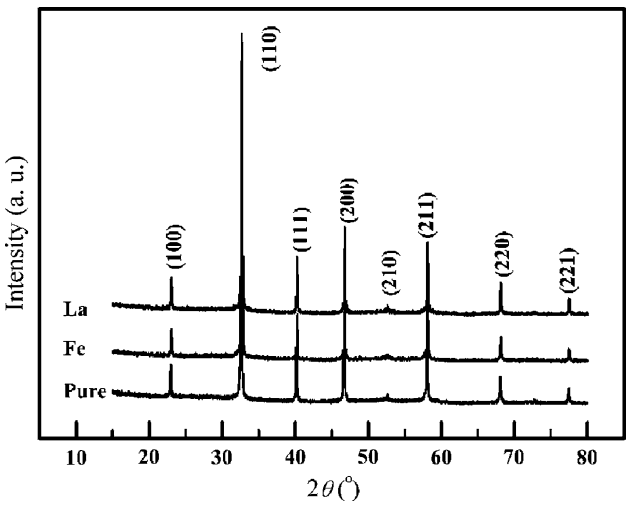

Fig. 1 X-ray diffraction patterns of the pure, Fe, and La-doped BNLBMT0.06 lead-free ceramics

Experimental

BNLBMT0.06 ceramics doped with 0.2 mol% Fe and La were prepared by a conventional solid state reaction method using Bi_2O_3 (99.0%), Na_2CO_3 (99.8%), Li_2CO_3 (98.0%), $BaCO_3$ (99.0%), TiO_2 (98.0%), MnO_2 (97.5%), Fe_2O_3 (99.0%), and La_2O_3 (99.95%) as the starting raw materials, which were all commercially supplied (Sinopharm Chemical Reagent Co., Ltd. of China). For each composition, the starting materials were weighed according to the stoichiometric formula and ball milled (Nanjing University Instrument Plant of China) for 6 h in ethanol. The dried slurries were calcined at 850 °C for 2 h and then ball milled again. The powders were subsequently pressed into green disks with a diameter of 15 mm and sintering was carried out at 1,170 °C for 2 h in covered alumina crucibles. To minimize the evaporation of the volatile elements Bi and Na, the disks were embedded in a powder of the same composition. Silver paste was coated on both sides of the sintered samples and fired at 650 °C for 0.5 h to form electrodes. The specimens for measurement of piezoelectric properties were poled in silicone oil bath with a dc field of 3–4 kV/mm at 50 °C for 15 min. All the electrical measurements were performed after ageing for at least 24 h.

The crystal structures of the crushed sintered ceramics were characterized by powder X-ray diffraction (D8 Focus, Germany) using Cu $K\alpha_1$ radiation. Dielectric constant and loss of the ceramics were measured using an automatic acquisition system with an impedance analyzer (Agilent 4294A, America) from 25 to 400 °C under a heating rate of 2 °C min^{-1}. The piezoelectric constant d_{33} of the poled samples was measured using a Berlincourt d_{33} meter

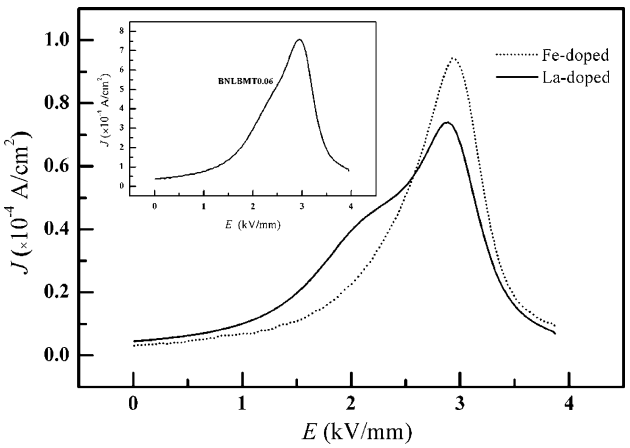

Fig. 2 The polarization current curves for the pure, Fe, and La-doped BNLBMT0.06 lead-free ceramics

(ZJ-3A, Institute of Acoustics, Chinese Academy of Science) at 55 Hz. The impedance spectrum for the radial and thickness extensional vibration modes were measured with Agilent 4294A analyzer to determine the resonance and antiresonance frequencies. The *J–E* curves, *P–E* loops, and *S–E* curves, where *J*, *P*, *E*, and *S* denote the polarization current density, polarization, the electric field and the strain, respectively, were measured in silicon oil at 0.1 Hz with the aid of a Sawyer–Tower circuit (TF2000 analyzer, Aixacct, Germany).

Results and discussion

The X-ray diffraction (XRD) patterns of the BNLBMT0.06 ceramics doped with Fe and La elements were measured under a scan step of 0.02° shown in Fig. 1. From Fig. 1 it can be observed that similar to the pure BNLBMT0.06 ceramic, the doped ceramics were both crystallized into a single-phase perovskite structure and no trace of second phase existed. Besides, in order to give an insight into the room-temperature phase, the XRD patterns with the 2θ range of 35°–48°, corresponding to the (111) and (200) diffraction peaks, were measured under a slower scanning step of 0.0025°. No characteristic peak splitting appeared, suggesting the pseudocubic structure at room temperature.

Figure 2 shows the polarization current density *J* as a function of the applied electric field for BNLBMT0.06 and doped ceramics. It can be observed that compared to the BNLBMT0.06 shown in the inset of Fig. 2, the peak values of the current density *J* were both greatly decreased to about one magnitude lower of about 0.8×10^{-4} A/cm^2 after doping. Figure 3 illustrates the room-temperature ferroelectric *P–E* loops and *S–E* curves of BNKBMT0.06 doped with Fe and La under an electric field of about 4 kV/mm at 0.1 Hz, respectively. From Fig. 3, typical rectangular loops can be observed for both ceramics. In comparison to the BNKBMT0.06 ceramics, the coercive field E_c of La-doped ceramic decreased from 2.63 to 2.46 kV/mm while that of Fe-doped one increased to 2.89 kV/mm. From the

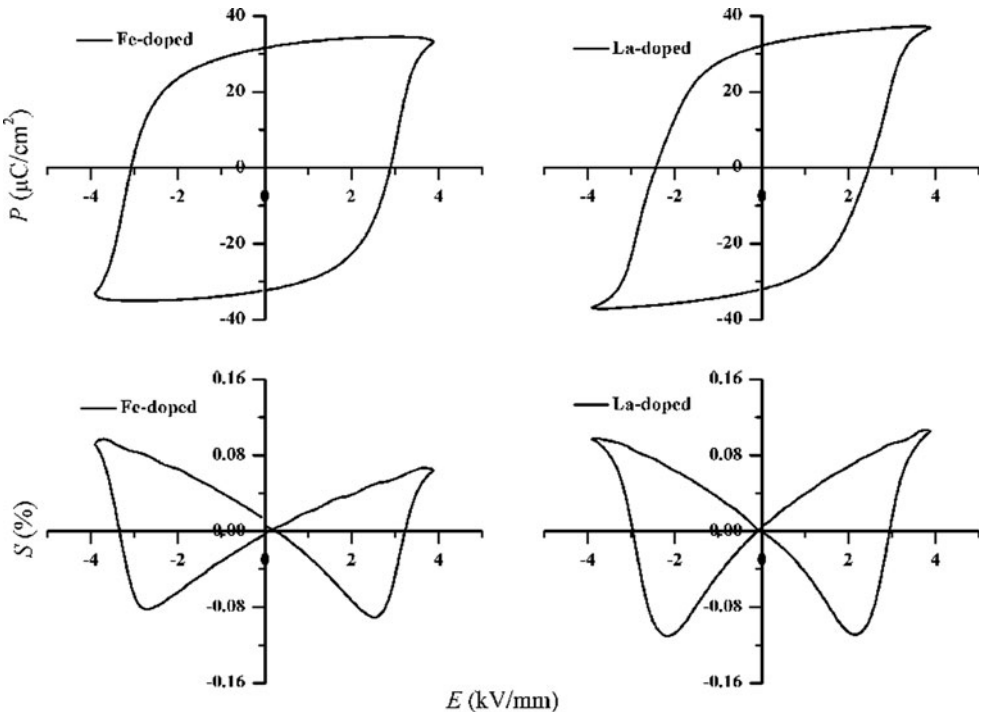

Fig. 3 Room-temperature ferroelectric *P–E* loops and bipolar *S–E* curves for the Fe and La-doped ceramics under the electric field of 4 kV/mm at 0.1 Hz

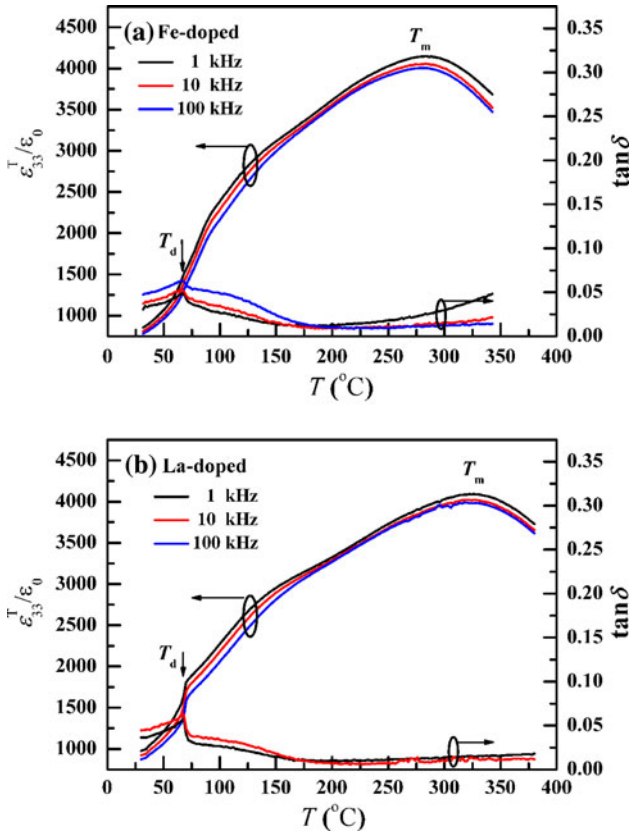

Fig. 4 Temperature dependence of the dielectric constant and loss for the **a** Fe-doped and **b** La-doped lead-free ceramics from 25 to 400 °C under the frequency of 1, 10, and 100 kHz

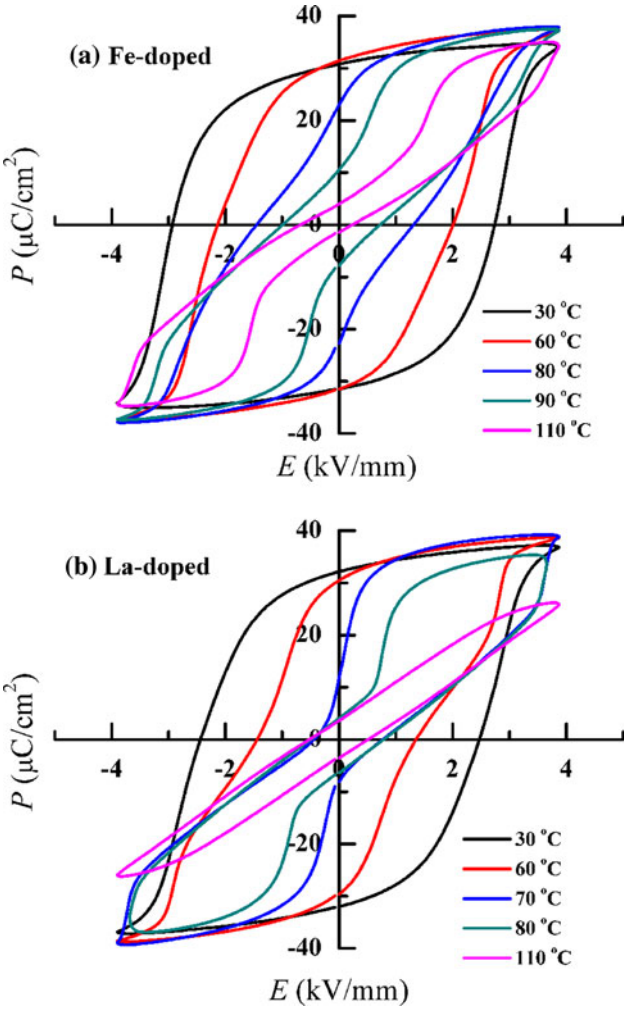

Fig. 5 Temperature dependence of the ferroelectric *P–E* loops for **a** Fe and **b** La-doped lead-free ceramics

S–E curves, typical butterfly curves can be observed for the La-doped ceramic. In comparison, the strain curve for the Fe-doped one exhibited weak asymmetric behavior and the reason for this will be discussed later.

In addition, the temperature dependence of the dielectric, ferroelectric, piezoelectric properties, and electric-field-induced phase transition behavior was also studied as shown in Figs. 4, 5, 6, 7, and 8. Figure 4a and b shows the frequency and temperature dependence of the dielectric constant $\left(\varepsilon_{33}^T/\varepsilon_0\right)$ and loss (tanδ) for the doped BNLBMT0.06 ceramics from 25 to 400 °C under the frequency of 1, 10, and 100 kHz. From the figures around the T_m, broad dielectric peaks could be observed, exhibiting relaxor characteristics with diffused phase transition behavior. This should be correlated with the multiple complexes in the A-site (such as Bi^{3+}, Na^{1+}, Ba^{2+}, Li^{+}, etc.) of perovskite compounds, which could lead to the compositional inhomogeneity in nanoscale [25]. The depolarization temperature T_d, determined from the peaks of the dielectric loss, is another important factor for BNT-based lead-free ceramics in view of their practical application. A comparison of the characteristic temperatures and the electrical properties between the pure and doped ceramics were summarized in Table 1. Compared to the pure ceramics, here the Fe-doped ceramic exhibits an improved mechanical quality factor (Q_m) ~ 160, E_c ~ 2.9 kV/mm and decreased loss tanδ ~ 0.024, indicating a hard characteristic while the La-doped one indicates a soft feature with increased d_{33} ~ 184 pC/N, $\varepsilon_{33}^T/\varepsilon_0 \sim 983$, tan$\delta$ ~ 0.033, and decreased E_c ~ 2.46 kV/mm.

Figure 5a and b illustrates the temperature dependence of the *P–E* loops for Fe and La-doped ceramics, respectively. From both loops, at room temperature the *P–E* exhibits typical rectangular loops, indicating strong ferroelectric order. With temperature increasing the loops became narrow and pinched hysteresis loops, which indicated the coexistence of the ferroelectric (FE) and antiferroelectric (AFE)-like behavior, appeared at certain critical temperature. The starting pinched temperature for Fe and La-doped ones can be determined to be about 80 and 70 °C, respectively, close to (actually slightly lower than) T_d measured from the dielectric data (Fig. 4a, b). With the temperature further

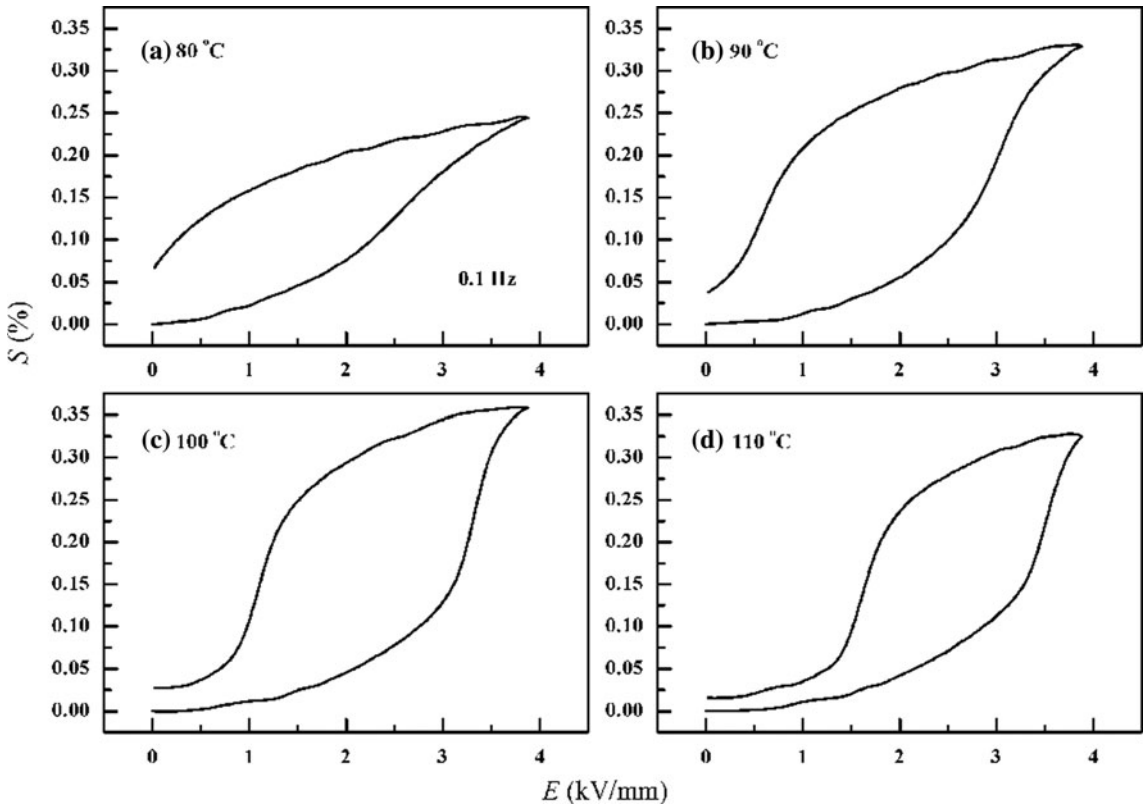

Fig. 6 The strain behavior under unipolar electric field for the Fe-doped ceramic at **a** 80 °C, **b** 90 °C, **c** 100 °C, and **d** 110 °C

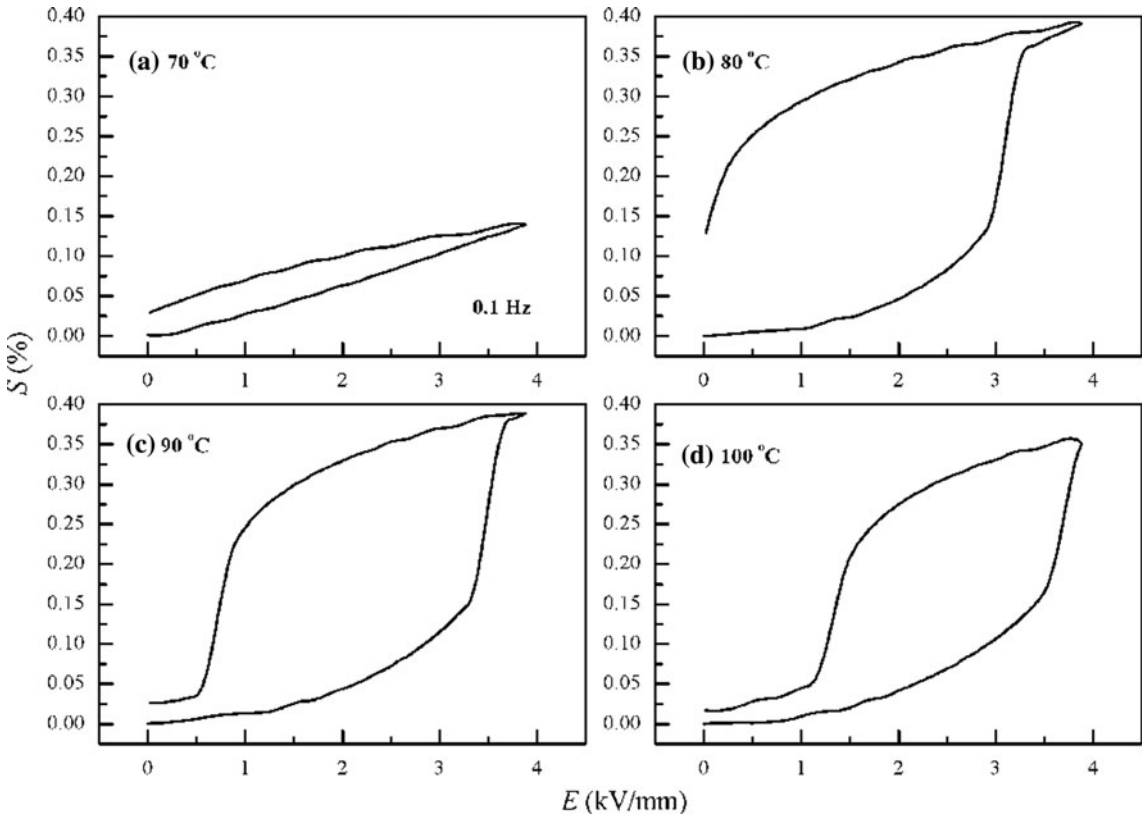

Fig. 7 The strain behavior under unipolar electric field for the La-doped ceramic at **a** 70 °C, **b** 80 °C, **c** 90 °C, and **d** 100 °C

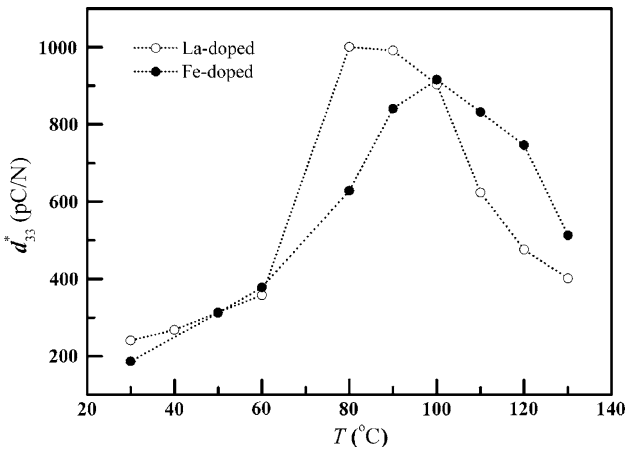

Fig. 8 Temperature dependence of the normalized piezoelectric constant d_{33}^* for Fe and La-doped lead-free ceramics

increasing, the AFE-like behavior became more obvious and the remnant polarization P_r and E_c decreased rapidly.

Figures 6 and 7 show the temperature dependence of the strain behavior under unipolar electric field. Below the depolarization temperature, little strain hysteresis can be observed under 4 kV/mm at 0.1 Hz. With the temperature increasing, nonlinear *S–E* response appeared, accompanied with ultrahigh maximum strain value. For the Fe-doped ceramics, the largest nonlinear response appeared at around 100 °C with the maximum strain of ~0.36%. For the La-doped one, the maximum value reached even higher of ~0.40% at around 90 °C, accompanied with a very large strain hysteresis. The temperature dependence of the normalized piezoelectric constant $\left(d_{33}^* = S_{max}/E_{max}\right)$ derived from the strain curves under unipolar electric field were summarized in Fig. 8. From Fig. 8, with the temperature increasing, the d_{33}^* both first increased to the maximum then decreased with temperature further increasing. The maximum values for the Fe and La-doped lead-free ceramics can reach as high as 915 and 1,000 pC/N, respectively. These d_{33}^* values were much larger than previously reported ones of the BNT-BT (~700 pC/N, at 100 °C) reported by Zhang et al. and Guo et al.'s results [24, 26].

For the increase in the $\varepsilon_{33}^T/\varepsilon_0$, tan$\delta$, and d_{33}, decrease in the E_c and Q_m obtained in La-doped ceramic, it is due to the similar radius between La^{3+} (1.36 Å) and perovskite A-site ions (Na^+ of 1.39 Å and Bi^{3+} of 1.34–1.36 Å) from Shannon's ionic radii [27]. The La^{3+} is more positive and the substitution will create A-site vacancies so as to facilitate the domain wall motions. On the other hand, the Fe^{3+} will substituted the Ti^{4+} and occupied the B-site due to similar ionic radius (Fe^{3+} of 0.65 Å and Ti^{4+} of 0.605 Å) [27], leading to the oxygen vacancies and created the internal bias field from the formation of the defect dipoles $\left(Fe'_{Ti} - V_O^{\cdot\cdot}\right)^{\cdot}$, which was always accompanied with asymmetric electric-field-induced strain behavior (Fig. 3). As a result, the material exhibited hard characteristics with lower $\varepsilon_{33}^T/\varepsilon_0$, loss tan$\delta$, and higher E_c [21]. Nevertheless, a decrease in the depolarization temperature T_d (from 76 to 68 °C) was unexpected in the Fe-doped ceramic and the reason responsible for this still need further study. Regarding the high strain response, Zhang et al. studied the large strain behavior in ternary solid solution $Bi_{0.5}Na_{0.5}TiO_3$–$BaTiO_3$–$K_{0.5}Na_{0.5}NbO_3$ (BNT–BT–KNN) and proposed that the mechanism was a field-induced AFE to FE phase transition and domain contribution [5, 28]. However, for an AFE-FE phase transition, a volume change should be always accompanied and Jo et al. excluded this assumption through simultaneously monitoring the longitudinal and transverse strain and attributed large strain response to the presence of the non-polar phase [8]. Hiruma et al. considered the high strain in $Bi_{0.5}Na_{0.5}TiO_3$–$SrTiO_3$ originated from the phase transition from pseudocubic (tetragonal) to rhombohedral accompanied with the rotation of the 180° and non-180° domains [29]. Quite recently, Eerd et al. reported a phase diagram of BNT-BT system in the range of 10–470 K through Raman spectroscopy [30]. Results indicated that with temperature increased to above T_d, the $(1 - x)$BNT-xBT with x lower than the MPB composition of 0.055 exhibited a short-range coherence (ferroelectric, instead of non-polar or antiferroelectric) with identical phase structure to that of BNT-BT with $x > 0.055$. In a word, up to present the intrinsic nature responsible for T_d is still quite controversial [8, 26, 30]. It is suggested that the large strain response around T_d in present study should be related to the development of the short-range order ferroelectric or non-polar phases slightly below T_d. When subjected to external electric field, these phases could generate a restoring force and bring the system back to its original state after field removal so as to realize high strain

Table 1 Electrical properties of pure, Fe and La-doped BNLBMT0.06 ceramics

	T_m (°C)	T_d (°C)	$\varepsilon_{33}^T/\varepsilon_0$	tanδ	d_{33} (pC/N)	k_p	k_t	Q_m	P_r (μC/cm^2)	E_c (kV/mm)
BNLBMT0.06	234	76	837	0.026	172	0.33	0.52	155	30.0	2.63
Fe doped	282	68	803	0.024	157	0.32	0.46	159	31.5	2.89
La doped	326	68	983	0.033	184	0.32	0.47	145	32	2.46

response. Similar results have also been observed in Zr-modified $Bi_{0.5}(Na_{0.78}K_{0.22})_{0.5}TiO_3$ system [31]. The high strain response obtained here provides a new way for applications under different temperature ranges.

Conclusions

In summary, acceptor Fe and donor La-modified BNLBMT0.06 ceramics were fabricated and the dielectric, ferroelectric, and piezoelectric properties were systematically characterized. The Fe-doped ceramic exhibited a hard effect with an increased Q_m and E_c, decreased $\varepsilon_{33}^T/\varepsilon_0$ and tanδ while the La-doped one indicated a soft feature with increased d_{33}, $\varepsilon_{33}^T/\varepsilon_0$, tan$\delta$, and decreased E_c. The intrinsic mechanism was briefly discussed. In addition, an ultrahigh electric-field-induced strain data with large normalized d_{33}^* up to $\sim$1,000 pC/N was obtained in the doped ceramics which was suggested ascribed to the formation of the short-range ferroelectric or non-polar phase at elevated temperature. The present study could also provide an important routine to obtain large strain response.

Acknowledgements This study was supported by the Science and Technology Commission of Shanghai Municipality (Grant No. 10ZR1422300 and 09520501000), Innovation Program of Shanghai Municipal Education Commission (09YZ151, 11YZ82, 11YZ83, and 11ZZ117), Shanghai Normal University Program (SK201026, PL929 and SK200708), National Natural Science Foundation of China (Grant No. 60807036), and Condensed Physics of Shanghai Normal University (Grant No. DZL712).

References

1. Jaffe B, Cook WR, Jaffe H (1971) Piezoelectric ceramics. Academic Press, London
2. Xu Y (1991) Ferroelectric materials and their applications. North-Holland Elsevier Science, Amsterdam
3. Directive 2002/95/EC of the European Parliament and of the Council of 27 January 2003, Official Journal of the European Union 2003, p. L37/19
4. Rödel J, Jo W, Seifert TPK, Anton EM, Granzow T, Damjanovic D (2009) J Am Ceram Soc 92:1153
5. Zhang ST, Kounga AB, Jo W, Jamin C, Seifert K, Granzow T, Rödel J, Damjanovic D (2009) Adv Mater 21:4716
6. Liu WF, Ren XB (2009) Phys Rev Lett 103:257602
7. Takenaka T, Nagata H, Hiruma Y (2008) Jpn J Appl Phys 47:3787
8. Jo W, Granzow T, Aulbach E, Rödel J, Damjanovic D (2009) J Appl Phys 105:094102
9. Shrout TR, Zhang SJ (2007) J Electroceram 19:111
10. Smolenskii GA, Isupov VA, Agranovskaya AI, Krainik NN (1961) Sov Phys-Solid State (Engl Transl) 2:2651
11. Zvirgzds JA, Kapostis PP, Zvirgzde JV (1982) Ferroelectrics 40:75
12. Jones GO, Thomas PA (2002) Acta Crystallogr B 58:168
13. Jones GO, Thomas PA (2000) Acta Crystallogr B 56:426
14. Nagata H, Yoshida M, Makiuchi Y, Takenaka T (2003) Jpn J Appl Phys 42:7401
15. Wang XX, Choy SH, Tang XG, Chan HLW (2005) J Appl Phys 97:104101
16. Shieh J, Wu KC, Chen CS (2007) Acta Mater 55:3081
17. Lin DM, Kwok KW, Chan HLW (2007) Solid State Ionics 178:1930
18. Yilmaz H, Trolier-Mckinstry S, Messing GL (2003) J Electroceram 11:217
19. Morozov MI, Damjanovic D (2008) J Appl Phys 104:034107
20. Morozov MI, Damjanovic D (2010) J Appl Phys 107:034106
21. Viehland D (2006) J Am Ceram Soc 89:775
22. Jo W, Erdem E, Eichel RA, Glaum J, Granzow T, Damjanovic D, Rödel J (2010) J Appl Phys 108:014110
23. Li JM, Wang FF, Qin XM, Xu M, Tang YX, Shi WZ (under review) J Alloy Compd
24. Zhang ST, Kounga AB, Aulbach E, Deng Y (2008) J Am Ceram Soc 91:3950
25. Smolenskii GA (1970) Jpn J Phys Soc Suppl 28:26
26. Guo YP, Liu Y, Withers RL, Brink F, Chen H (2011) Chem Mater 23:219
27. Shannon RD (1976) Acta Crystallogr A A32:751
28. Zhang ST, Kounga AB, Aulbach E, Granzow T, Jo W, Kleebe HJ, Rödel J (2008) J Appl Phys 10:034107
29. Hiruma Y, Imai Y, Watanabe Y, Nagata H, Takenaka T (2008) Appl Phys Lett 92:262904
30. Eerd BW, Damjanovic D, Klein N, Setter N, Trodahl J (2010) Phys Rev B 82:104112
31. Hussain A, Ahn CW, Lee JS, Ullah A, Kim IW (2010) Sens Actuators A 158:84